

Texture in stainless steel welds: an ultrasonic study

H. M. LEDBETTER, M. W. AUSTIN

Fracture and Deformation Division, National Bureau of Standards, Boulder, Colorado 80303, USA

We studied texture effects in five AISI-316 stainless-steel welds. We measured nine independent ultrasonic velocities along the weld's principal axes. These velocities reveal a strong texture different from the $\langle 001 \rangle$ fibre-type usually attributed to these materials. The texture is independent of delta-ferrite content and must contain a strong $\langle 110 \rangle$ component related to the f c c monocystal elastic constant $C' = (C_{11} - C_{12})/2$. A postulated ideal $(001)[110]$ plate-type texture explains the range of measured longitudinal and transverse sound velocities, but not their detailed values.

1. Introduction

Most metal processing produces texture, a non-random distribution of crystallite orientations in a polycrystal. Well-known processes that produce texture include: mechanical deformation, annealing (recrystallization), solidification, electrodeposition, vapour deposition (epitaxy), phase transformation, and welding. In each case, one can identify a gradient (mechanical, thermal, electrical, and so forth) that favours one crystal orientation over another.

Texture induces anisotropic macroscopic physical and plastic properties. Thus, usual polycrystal-monocystal relationships for quasi-isotropic (nontextured) aggregates provide only a rough guess for the macroscopic material properties. A better guess must include information concerning the orientation-distribution function of the crystallites.

In principle, any property affected by texture provides a possible tool for probing texture. For example: electrical resistivity, thermal expansivity, thermal conductivity, and so forth. But, these particular properties, which one represents as second-rank tensors, cannot work for the cubic-symmetry case where they are direction-independent, texture-independent scalars.

A texture-probing physical property useful for all crystal-symmetry cases, including cubic, is the elastic-stiffness tensor. For the cubic case it con-

tains three independent components: usually C_{11} , C_{12} and C_{44} in Voigt's contracted notation. Below, we consider the sound velocity, $v = (C/\rho)^{1/2}$, where ρ denotes mass density. In general, sound velocities are roots of the Christoffel equations:

$$\det(C_{ijkl}x_jx_k - \rho v^2\delta_{il}) = 0 \quad (1)$$

where C_{ijkl} denotes the full fourth-rank elastic-stiffness tensor, x_j denotes components of the unit wave vector relative to cubic axes, and δ_{il} denotes the Kronecker delta. Thus, in an anisotropic medium, v depends on direction according to the elastic constants of the medium. Thus, in principle, one can determine the symmetry and the orientation of an anisotropic elastic body by measuring v in various directions.

In practice, one seldom uses physical properties to study texture; one usually uses X-ray diffraction. Two references summarize the phenomenology of texture and the X-ray diffraction approach: Wasserman and Grewen [1] and Barrett [2]. A single source dominates the description of mathematical texture-analysis: Bunge [3], which contains 302 references.

The present study used elastic constants, or, equivalently, sound velocities, to examine the texture in AISI-316 stainless-steel welds. These welds contained up to 10 vol% delta-ferrite. Besides determining the delta-ferrite effect, this study provides information on the anisotropic

TABLE I Chemical compositions (wt %), balance iron

Specimen	Cr	Ni	Mo	Mn	C	N	Nb	Si	S	P
1	18.47	13.97	2.25	1.72	0.031	0.042	0.14	0.58	0.011	0.033
2	18.64	12.97	2.29	1.72	0.020	0.046	0.14	0.56	0.012	0.034
3	19.20	12.01	2.32	1.70	0.034	0.042	0.15	0.57	0.009	0.034
4	19.66	11.06	2.18	1.76	0.028	0.067	0.15	0.59	0.008	0.029
5	18.69	12.85	2.25	1.75	0.059	0.044	0.15	0.56	0.009	0.033

elastic constants of these welds. This information serves several purposes: determination of residual stress; calculation of optimum (lowest attenuation) stress-wave direction for ultrasonic study of flaws (using either body waves or surface waves); material characterization; and characterization of the weld process.

2. Materials

From a commercial source, we obtained welds in the form of 2.5 cm plates of AISI-316 stainless steel. These were welded by a shielded-metal-arc process under the following conditions: E316L electrode, 30 A, 24 V, 15 to 20 cm min⁻¹ travel speed, 93 to 212°C interpass temperature, 25 to 33 passes. Table I gives chemical compositions. Table II gives some metallurgical properties. Further material characterization together with some mechanical-property measurements were given by Read *et al.* [4].

We prepared specimens for ultrasonic study by cutting, grinding, and polishing using usual metallographic procedures. These specimens were rectangular prisms measuring approximately 2.5 cm × 2.5 cm × 0.3 to 0.5 cm.

3. Sound-velocity measurements

Longitudinal-mode and transverse-mode sound velocities were determined by a pulse-echo method described in detail previously [5]. Briefly, rectangular prisms were prepared by grinding so that opposite faces were flat and parallel within 5 μm. Quartz piezoelectric crystals with fundamental resonances between 4 and 7 MHz were cemented with phenyl salicylate to the specimens. An x-cut

transducer was used for longitudinal waves and an ac-cut for transverse waves. Ultrasonic pulses 1 to 2 cycles long were launched into the specimen by electrically exciting the transducer. The pulses propagated back and forth. The pulse echoes were detected by the transducer and displayed on an oscilloscope equipped with a time delay and a microprocessor for time-interval measurements. The sound velocity was computed by

$$v = 2l/t \quad (2)$$

where l denotes specimen length, and t the round-trip transit time. On the oscilloscope, t was the time between adjacent echoes, the first and second echoes usually being measured, and within these echoes the time between leading cycles. Elastic constants were computed from the general relationship

$$C = \rho v^2 \quad (3)$$

where ρ denotes mass density.

Extensional-mode sound velocities were determined by a Marx-oscillator method described elsewhere [6]. These measurements lead directly to Young's modulus via the relationship

$$E = 4\rho f^2 l^2 \quad (4)$$

where f denotes specimen resonance frequency and l denotes specimen length.

4. Results

Fig. 1 shows measured sound velocities against ferrite content. In this figure, the first subscript indicates wave-propagation direction and the second indicates polarization direction. The dashed lines in Fig. 1 indicate the longitudinal and transverse sound velocities for nontextured 316 stainless steel [7]. The coordinate system is: x_3 perpendicular to welded plate, x_1 along weld direction, x_2 orthogonal to x_1 and x_3 . For specimen 5, Table III gives eight sound velocities; v_{23} could not be determined accurately and is not reported. (We assume $v_{23} = v_{32}$.) The laboratory units, cm μsec⁻¹, convert to m sec⁻¹ when multi-

TABLE II Metallurgical properties

Specimen	Ferrite (vol %)	WRC ferrite number	Mass density (g cm ⁻³)
1	0.13	0.12	7.932
2	4.1	4.5	7.934
3	8.5	9.2	7.921
4	10.1	11.0	7.910
5	1.2	1.3	7.930

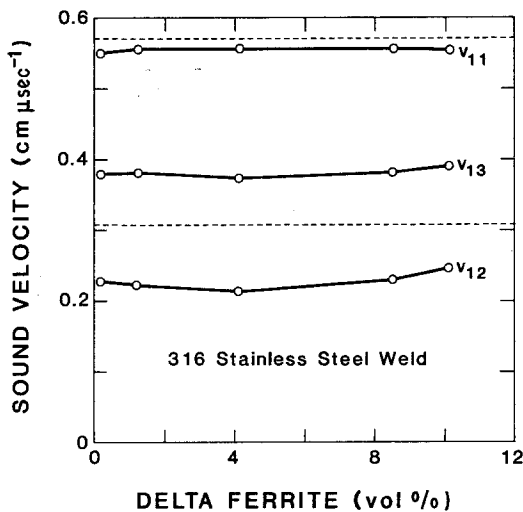


Figure 1 Longitudinal and transverse sound velocities against delta-ferrite content for 316-stainless-steel welds. Dashed lines indicate isotropic (nontextured) velocities: upper = longitudinal, lower = transverse.

plied by 10^4 . The set of nine velocities v_{ij} ($i, j = 1, 2, 3$) correspond to all possible waves propagated and polarized along the principal axes x_1, x_2 and x_3 . We measured no off-axis sound velocities. Also for specimen 5, the Young's modulus results were $E_3 = 1.52$ and $E_2 = 1.20 \times 10^{11} \text{ N m}^{-2}$. Our specimens were too short along x_1 to permit measurement of E along the weld direction.

5. Discussion

Fig. 1 shows that the sound velocities and, therefore, the elastic constants of these stainless-steel welds do not vary strongly with composition. This suggests that the elastic constants of delta-ferrite do not differ significantly from those of austenite. This is hardly surprising because the atomic volumes of the two phases differ by only one or two per cent. Also, Ledbetter and Reed [8] showed for Fe-Ni alloys that the alpha-ferrite and austenite elastic constants do not differ dramatically.

For all cases, the longitudinal sound velocity v_{11} falls below the isotropic (nontextured) value, 0.569. This suggests the existence of texture in all the specimens. It is consistent with the $\langle 001 \rangle$ fibre texture often suggested for these welds [9].

TABLE III Sound velocities in specimen 5 in units of $\text{cm } \mu\text{sec}^{-1}$

$v_{11} = 0.555$	$v_{22} = 0.568$	$v_{33} = 0.538$
$v_{12} = 0.222$	$v_{21} = 0.260$	$v_{31} = 0.363$
$v_{13} = 0.381$	$(v_{23} = 0.387)$	$v_{32} = 0.387$

Ledbetter [10] calculated that a pure $\langle 001 \rangle$ fibre texture requires $v_{11} = 0.510$.

One expects that cubic-symmetry crystallites in welds occur either with random orientations or with a single preferred axis parallel to the principal heat-flow direction, denoted x_3 . In the x_1 - x_2 plane, crystallites are expected to orient themselves randomly because no preferred heat-flow direction occurs in that plane. Thus, an effective fibre texture occurs with x_3 being the fibre axis. Macroscopically, such a material exhibits transverse-isotropic symmetry, with five independent elastic constants. This is equivalent to hexagonal symmetry. In Voigt's contracted C_{ij} notation the symmetrical elastic-stiffness matrix is

$$C_{ij}^H = \begin{bmatrix} C_{11}^H & C_{12}^H & C_{13}^H & 0 & 0 & 0 \\ & C_{11}^H & C_{13}^H & 0 & 0 & 0 \\ & & C_{33}^H & 0 & 0 & 0 \\ & & & C_{44}^H & 0 & 0 \\ & & & & C_{44}^H & 0 \\ & & & & & C_{66}^H \end{bmatrix} \quad (5)$$

where $C_{66}^H = \frac{1}{2}(C_{11}^H - C_{12}^H)$. Thus, the theoretical problem is to express the five hexagonal-symmetry elastic constants, C_{ij}^H , in terms of the three cubic-symmetry elastic constants: C_{11}, C_{12}, C_{44} .

The present theory does not permit calculation of the elastic constants of textured polycrystalline aggregates of cubic-symmetry crystallites. This is a special and more difficult case of determining the average elastic constants of a random polycrystalline aggregate. For this latter problem, Landau and Lifshitz [11] remind us that "there is ... no general relationship between the moduli of elasticity of a polycrystal and those of a single crystal of the same substance." The fibre-texture case involves a two-dimensional, rather than a three-dimensional, average.

However, elastic-constant "bounds" can be calculated for textured aggregates. In this study we calculate the Voigt (constant strain) and Reuss (constant stress) bounds and use Hill's suggestion of an arithmetic average to estimate the elastic constants. This approach turns out to be quite reasonable because the Voigt and Reuss bounds do not differ dramatically (a maximum of 37 per cent). And for the important $\langle 001 \rangle$ texture case, the bounds coincide for three elastic constants: C_{13}^H, C_{33}^H and C_{44}^H . Thus, we know these three

constants unambiguously. Kröner and Wawra [12] explain the systematics of this bounds coincidence, and they give the following expressions for the C_{ij}^H :

$$\begin{aligned} C_{11}^H &= C_1 + 3\beta C_3 = \frac{1}{4}(3C_{11} + C_{12} + 2C_{44}) \\ C_{12}^H &= C_2 + \beta C_3 = \frac{1}{4}(C_{11} + 3C_{12} - 2C_{44}) \\ C_{13}^H &= C_2 - 4\beta C_3 = C_{12} \\ C_{33}^H &= C_1 = 8\beta C_3 = C_{11} \\ C_{44}^H &= \frac{1}{2}(C_1 - C_2) - 4\beta C_3 = C_{44} \\ C_{66}^H &= \frac{1}{2}(C_{11}^H - C_{12}^H) = \frac{1}{4}(C_{11} - C_{12} + 2C_{44}) \end{aligned} \quad (6)$$

where

$$\begin{aligned} 5C_1 &= 3C_{11} + 2C_{12} + 4C_{44} \\ 5C_2 &= C_{11} + 4C_{12} + 2C_{44} \\ C_3 &= C_{11} - C_{12} - 2C_{44} \end{aligned} \quad (7)$$

where $\beta = 1/20$ for $\langle 100 \rangle$ fibre texture.

Correct relationships for the S_{ij} , which give the Reuss bounds by matrix inversion, appear only once [13] in the literature. These are

$$\begin{aligned} S_{11}^H &= \frac{1}{8}(6S_{11} + 2S_{12} + S_{44}) \\ S_{12}^H &= \frac{1}{8}(2S_{11} + 6S_{12} - S_{44}) \\ S_{13}^H &= S_{12} \\ S_{33}^H &= S_{11} \\ S_{44}^H &= S_{44} \\ S_{66}^H &= 2(S_{11}^H - S_{12}^H) = S_{11} - S_{12} - S_{44}/2. \end{aligned} \quad (8)$$

In deriving these relationships, one must remember that the inverse C_{ijkl}^{-1} of a fourth-rank elasticity tensor relates to the inverse $C_{\alpha\beta}^{-1}$ of its associated 6×6 matrix by a factor multiplied times C_{ijkl}^{-1} . This factor is 4 if both α and β exceed 3, is 2 if either α and β exceeds 3, and is 1 if neither α nor β exceeds 3.

The most dramatic result of our measurements, as shown in Fig. 1, is the splitting of the isotropic $v_{13} = v_{12} = 0.307$ shear velocity into two velocities $v_{13} = 0.381$ and $v_{12} = 0.228$ (average of five). One expects the shear-wave birefringence to provide a more sensitive probe of texture than the smaller shift in the longitudinal velocity. This arises because, even for highly anisotropic cubic crystals, v_l depends only slightly on direction [14]. However, this particular v_t splitting is inconsistent with a $\langle 001 \rangle$ fibre texture for which Ledbetter [10] showed that the two velocities should be

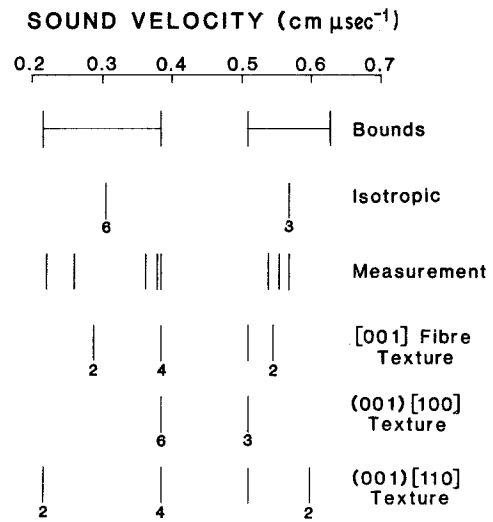


Figure 2 Longitudinal and transverse sound velocities for 316-stainless-steel welds. Small numerals indicate n -fold degeneracy.

0.384 and 0.289. That is, $v_{12} = 0.228$ is much too low for a $\langle 001 \rangle$ fibre texture.

Departure of measurement from a $\langle 001 \rangle$ fibre texture is shown schematically in Fig. 2. At the top, Fig. 2 gives the bounds of Voigt (upper) and Reuss (lower). Any type of texture in any amount must produce velocities within these bounds. Our measurements meet this criterion. For the shear mode, we found velocities very close to both the upper and lower bounds, which correspond to C_{44} and to $C' = (C_{11} - C_{12})/2$, respectively. Thus, the fcc monocrystalline C_{44} and C' must be two of the principal elastic constants of the textured aggregate. Again, the often-suggested $\langle 000 \rangle$ fibre texture fails as a possible texture because its elastic constants contain C_{44} but not C' . If we assume another texture component, $\langle 100 \rangle$ in the weld direction, which amounts to a $(001)[100]$ texture, the situation worsens, as Fig. 2 shows. The situation improves if we assume $\langle 110 \rangle$ in the weld direction; this amounts to a $(001)[110]$ texture. Fig. 2 shows that this ideal texture explains the range of shear velocities, but not the detailed measurements without some perturbations. Possible perturbations included partial texture, a second texture, and deviations from a (001) plane or a $[110]$ direction (or both).

6. Summary

The present study produced the following conclusions concerning the elastic constants and

sound velocities of AISI-316 stainless-steel welds:

1. Up to at least 10 vol% delta-ferrite content, the elastic constants are independent of ferrite content.

2. All specimens exhibit texture and significant departures from quasi-isotropic physical-property values. The texture is independent of ferrite content.

3. For these materials, the usual model, $\langle 001 \rangle$ fibre texture, fails to explain the measurements.

4. Calculated results for several other textures show that the elastic constant $C' = (C_{11} - C_{12})/2$, or a $[110]$ texture element, enters essentially into the weld's texture.

5. A postulated texture — $(001)[110]$ — covers the range of eight measured sound velocities, but not the details of their distribution. Some other, presently unknown, element of texture must also occur.

Acknowledgement

This study arose from research sponsored by the US DoE Office of Fusion Energy.

References

1. G. WASSERMAN and J. GREWEN, "Texturen metallischer Werkstoffe" (Springer-Verlag, Berlin, 1962).
2. C. S. BARRETT, "Structure of Metals" (McGraw-Hill, New York, 1952) pp. 442–520.
3. H. J. BUNGE, "Texture Analysis in Materials Science" (Butterworths, London, 1982).
4. D. T. READ, H. J. McHENRY, P. A. STEINMEYER and R. D. THOMAS, *Weld Res. J. Suppl.* **59** (1980) 104s.
5. H. M. LEDBETTER, N. V. FREDERICK and M. W. AUSTIN, *J. Appl. Phys.* **51** (1980) 305.
6. H. M. LEDBETTER, *Cryogenics* **20** (1980) 637.
7. *Idem*, *Met. Sci.* **14** (1980) 595.
8. H. M. LEDBETTER and R. P. REED, *J. Phys. Chem. Ref. Data* **2** (1973) 531.
9. B. R. DEWEY, L. ADLER, R. T. KING and K. V. COOK, *Exper. Mech.* **17** (1977) 2.
10. H. M. LEDBETTER, in "Review of Progress in Quantitative Nondestructive Evaluation", Vol. 1 (Plenum Press, New York, 1982) p. 619.
11. L. D. LANDAU and E. M. LIFSHITZ, "Theory of Elasticity" (Pergamon Press, London, 1959) p. 40.
12. E. KRÖNER and H. H. WAWRA, *Phil. Mag.* **A38** (1978) 433.
13. C. M. SAYERS, *ibid.* **A47** (1983) L1.
14. H. M. LEDBETTER and R. L. MOMENT, *Acta Metall.* **24** (1976) 891.

*Received 22 March
and accepted 4 June 1984*